Copyright © 2011 American Scientific Publishers
All rights reserved
Printed in the United States of America

Journal of Nanoscience and Nanotechnology
Vol. 11, 458–462, 2011

Influence of Synthesis Temperature on the Properties of Ga-Doped ZnO Nanorods Grown by Thermal Evaporation

Cheol Hyoun Ahn, Young Yi Kim, and Hyung Koun Cho*

School of Advanced Materials Science and Engineering, Sungkyunkwan University, 300 Cheoncheon-dong, Jangan-gu, Suwon, Gyeonggi-do, 440-746, Korea

This study examined the effect of the synthesis temperatures on the characteristics of vertically aligned Ga-doped ZnO (GZO) nanorods grown on a ZnO template by thermal evaporation using Zn and Ga sources. The increase in synthesis temperature at less than 700 °C induced stress relaxation relative to the ZnO template due to the suppression of defect generation by the formation of nanorods, while a further increase resulted in an increase in compressive strain due to dominant Ga doping. The increase in Ga concentration in the GZO nanorods with increasing synthesis temperature was also confirmed by X-ray photoelectron spectroscopy and photoluminescence. The best conductivity was observed in the GZO nanorods grown at 800 °C. On the other hand, the GZO nanorods synthesized at 900 °C showed less conductivity and weak near-band-edge emission properties due to the generation of defects from the excess Ga.

Keywords: Nanorods, Ga-Doped, Thermal Evaporation, Catalyst Free.

Delivered by Ingenta to:
Sung Kyun Kwan University
IP : 115.145.205.35
Mon, 10 Jan 2011 00:24:17

1. INTRODUCTION

Zn-based wide-band gap oxide semiconductors with superior physical properties, such as intense emission, chemical and thermal stability, transparency, and wide electrical conductivity range, have demonstrated their potentials in wide range of applications including ultraviolet laser diodes (LDs),[1] lighting-emission-diodes (LEDs),[2] transparent thin-film transistors,[3] sensor devices,[4] and piezoelectrics.[5] In particular, one-dimensional (1D) ZnO nanostructures are expected to show unique physical phenomenon and high efficiency characteristics due to the increased surface to volume ratio and quantum confinement effects.[6] However, the increase in electrical conductivity of ZnO nanorods is vital to achieve high efficiency optoelectronic devices and their commercial purposes. The control of the electrical properties by changes in intrinsic defects in un-doped ZnO is unstable and not reproducible. In this context, the electrical conductivity of 1D ZnO nanostructures can be enhanced by extrinsic doping using group III metals such as Al, Ga, In, etc.[7–10] Among these various dopant metals, Ga is a useful element, because it has a similar ionic (0.62 Å) and covalent radius (1.26 Å) to Zn (0.74 Å and 1.31 Å, respectively), which is in contrast to In (0.81 Å, 1.44 Å) and Al (0.5 Å, 1.26 Å).[11] Moreover, Ga doped ZnO (GZO) shows good electrical conductivity and transparency in the films grown by vacuum deposition.[12] Additionally, Ga-doped ZnO exhibited greater resistant to oxidation, suggesting higher chemical stability compared to undoped ZnO.

However, heavy doping would lead to degrade the structural, electrical, and optical properties of the ZnO nanorods.[13–15] Though, thermal evaporation is a simple and cost effective method of synthesizing 1D ZnO nanostructures, different evaporation rates for source materials make uniform doping in the ZnO nanorods more complicated. Thus, Ga with different evaporation efficiency from that of Zn requires elaborate control of the synthesis conditions. Therefore, it would be interesting to examine the effects of the synthesis temperatures on electrical and chemical properties of GZO nanorods. In this study, GZO nanorods were synthesized on a ZnO template by thermal evaporation at various temperatures, and their chemical, structural, electrical, and optical properties were investigated.

2. EXPERIMENTAL DETAILS

Ga-doped ZnO (GZO) nanorods were synthesized by simple thermal evaporation method at various temperatures.

*Author to whom correspondence should be addressed.

RESEARCH ARTICLE

1533-4880/2011/11/458/005 doi:10.1166/jnn.2011.3196

To fabricate vertically arrayed nanorods, 400 nm thick ZnO templates, which were deposited on *n*-Si by radio-frequency (RF) magnetron sputtering, were used as a seed layer. After forming the template layers, the Ga incorporated ZnO nanorods were synthesized in a horizontal tube furnace using Zn and Ga metal powders of 1:1 ratio. Ar was used as a carrier gas for the metal vapors and the reactor pressure was maintained at 5 Torr during synthesis. The synthesis temperatures were changed from 600∼900 °C. The effects of the Ga source contents on the formation of the GZO nanorods reported elsewhere.[13] The ratio of the Ga and Zn sources was fixed to 1:1, which is the condition showing better electrical performance.

The chemical, structural, and optical properties of the GZO nanorods synthesized at various temperatures were examined by X-ray photoelectron spectroscopy (XPS), X-ray diffraction (XRD), and photoluminescence (PL), respectively. The I–V characteristics of the GZO nanorods were determined using a Keithley millimeter. For the electrical measurements, the gaps between the GZO nanorods were filled with insulating polyimide. The top region of the polyimide filled nanorods was exposed by reactive ion etching (RIE), and then the Au/Ti bilayer electrodes were deposited as an electrode.

3. RESULTS AND DISCUSSION

Delivered by Ingenta to:
Sung Kyun Kwan University
IP: 115.145.205.35
Mon, 10 Jan 2011 00:24:17

Figure 1 shows SEM images of the vertically aligned Ga-doped ZnO (GZO) nanorods synthesized by thermal evaporation at various temperatures. The GZO nanorods synthesized by the template-assisted method show perfect vertical arrays at more than 600 °C. The length of the GZO nanorods increased continuously from 3.5 to 6.7 μm with increasing growth temperature up to 800 °C due to the increase in vapor-transfer density. However, further increase in temperature to 900 °C resulted in the reduction of length to 1.1 μm due to the enhanced re-evaporation rate of source materials at high temperatures. In addition, the diameter of the nanorods was also increased, as shown in the insets of Figure 1. This indicates that an increase in growth temperature to 800 °C induces significant enhancement in the number of the adatoms deposited from travelling vapor. The ZnO films on Si substrates are believed to show the growth behavior of 3D islands in order to minimize of the stress-related energy in the initial growth stage due to the large lattice mismatch with the substrate. The ZnO templates grown on Si substrates received compressive stress with respect to bulk ZnO, which originates from the residual misfit stress and subsequent cooling-down process by the large thermal coefficient mismatch.[16] In addition, Shin et al.[17] suggested that the high density of defects, such as grain boundaries, dislocations, and stacking faults observed in the polycrystalline ZnO thin film on the Si substrates is considered as another reason for the compressive stress. In contrast, the un-doped ZnO nanorods on the ZnO template showed reduced stress, which is considered to result from the absence of grain boundaries and dislocations by the formation of perfect single crystal nanorods without defects, as shown in region I in Figure 2. The stress in the nanorods becomes more relaxed with the incorporation of Ga. In particular, the GZO nanorods synthesized at 700 °C are almost stress-free. It is well known that the incorporation of Ga in the ZnO matrix induces a decrease in the lattice constant, because the covalent bond length of Ga–O (0.192 nm) is smaller than that of Zn–O (0.197 nm).[11] However, the

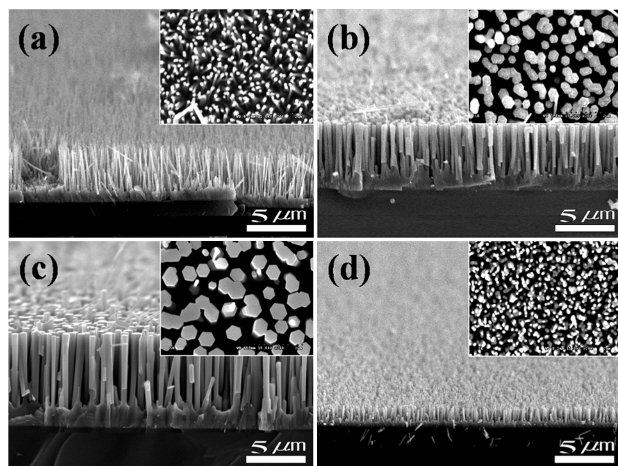

Fig. 1. SEM images of the GZO nanorods synthesized at various temperatures; (a) 600, (b) 700, (c) 800, and (d) 900 °C. The insets show plan-view SEM images observed under the same magnification.

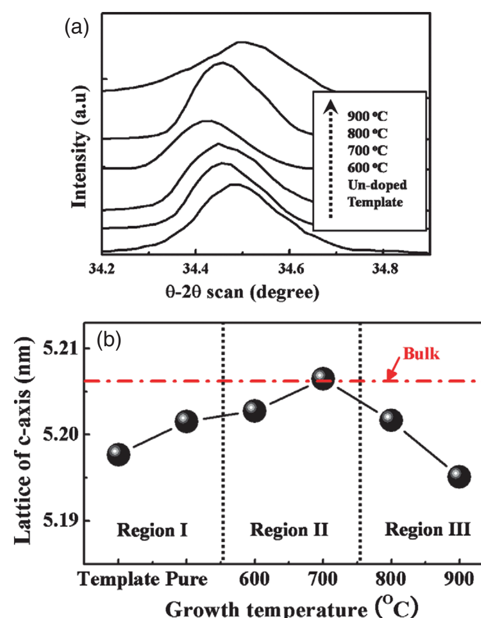

Fig. 2. (a) XRD spectra of (0002) diffraction peaks obtained from the template, undoped ZnO nanorods, and GZO nanorods. (b) Change in c-axis lattice constants as a function of the growth temperature. The results of the template and un-doped ZnO nanorods are included for comparison.

RESEARCH ARTICLE

behavior of the GZO nanorods in region II showed an opposite trend. The stress reduced by the increase in lattice constant of the GZO nanorods in region II was attributed to the elimination of grain boundaries and dislocations, which means that stress increment is more dominant than the decrease in the lattice constant by the incorporation of Ga. At synthesis temperatures ≥700 °C, the GZO nanorods showed increased compressive strain due to the smaller radius of the Ga atom than Zn atom. Consequently, it is expected that a high synthesis temperature assists in the production of conducting nanorods due to the incorporation of electrical dopants.

The distribution of Ga in the nanorods was examined by determining the chemical bonding properties of the GZO nanorods synthesized at various temperatures by XPS, as shown in Figure 3. As shown in Figure 3(a), the GZO nanorods fabricated at 600 °C showed only two Zn related peaks at 1111 and 1024 eV corresponding to Zn $2P_{3/2}$ and Zn $2P_{1/2}$ in the ZnO system. However, the GZO nanorods at elevated temperatures of >600 °C clearly showed additional Ga $2P_{3/2}$ and Ga $2P_{1/2}$ peaks in the spectrum, in which the intensity of the Ga related peaks increased with increasing growth temperature. This suggests that synthesis using Zn and Ga sources at high temperatures induces the fabrication of Ga incorporated GZO nanorods with vertical arrays on the ZnO templates. Figure 3(b) shows the asymmetric O 1s peaks of the GZO nanorods fitted by two Gaussian peaks. Based on previous XPS analysis of ZnO thin films,[18] the higher binding energy corresponding to 531.4∼532 eV related to the O 1s peak of XPS is normally assigned to an oxygen-deficiency, while the lower binding energy of 529.8∼530.5 eV resulted from the O^{2-} ions in the ZnO wurtzite structure. Interestingly, with increasing growth temperature, the intensity of the O 1s peak related to oxygen vacancies in the GZO nanorods decreased with increasing intensity of the O^{2-} ions related peak, together with an increase in the peak intensity for Ga–O bonding. It shows that an increase in synthesis temperature enhances the replacement efficiency of Ga atoms in the Zn sites, resulting in the suppression of oxygen vacancy sites. It is generally believed that ZnO nanorods synthesized using vapor transition methods at high temperatures have a high density of oxygen vacancies. In particular, the density of oxygen vacancies increased with increasing in synthesis temperature. However, the Ga–O bond, which has a covalent bond length slightly smaller than that of Zn–O, inhibited the formation of oxygen vacancies, even though synthesis occurred at high temperatures. Therefore, the incorporation of Ga in ZnO nanorods is expected to show a low density of oxygen vacancies and conducting properties due to substitution of Ga atoms in Zn sites.

Figure 4 shows the low-temperature (10 K) PL spectra on the GZO nanorods synthesized at various temperatures. With increasing temperature, the FWHM of near band edge (NBE) emission in the GZO nanorods was broadened from 40.9 to 66.6 meV (Fig. 4(a)). In general, when dopants such as Al, In, and Ga were included, the PL line broadening may be the result of doping charge fluctuations.[19] Moreover, the extent of PL line broadening increases with increasing doping concentration, which is consistent with the XPS and XRD results. Furthermore, the peak position of NBE emission shifted toward higher photon energy with improved NBE intensity with increasing growth temperature up to 800 °C. This behavior is related to the well-known Burstein-Moss (BM) effect. However, a further increase in growth temperature to 900 °C induced

Delivered by Ingenta to:
Sung Kyun Kwan University
IP: 115.145.205.35
Mon, 10 Jan 2011 00:34:17

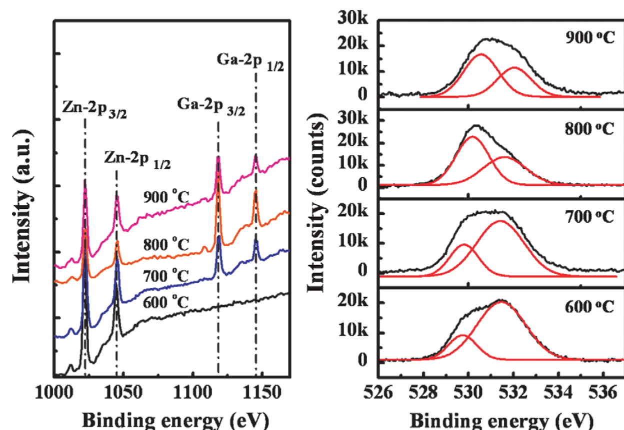

Fig. 3. XPS results of the GZO nanorods synthesized at various temperatures; (a) XPS peaks corresponding to Zn 2p and Ga 2p peaks, (b) XPS peak for O 1s. The asymmetric O 1s peaks are fitted by two Gaussian peaks.

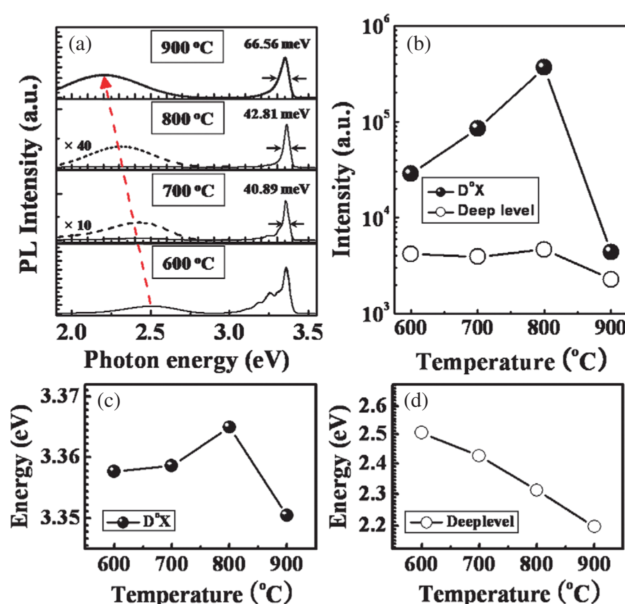

Fig. 4. (a) Low temperature (10 K) PL spectra of the GZO nanorods synthesized at various temperatures. (b) Intensity variation in NBE emission and deep-level emission as a function of the synthesis temperature. (c) and (d) variation in peak position of NBE emission and deep-level emission, respectively.

a shift of peak position to lower energy and a decrease in emission intensity, as shown in Figure 4. The relative intensity of deep level emission in the visible region to that of NBE also decreased up to growth temperature of 800 °C, and further increases in temperature resulted in an increase in the contribution from deep level emission (Fig. 4(b)). Although low Ga doping in ZnO does not contribute to the creation of the defects responsible for deep-level emission, the excessive incorporation of Ga atoms can promote the formation of lattice defect complexes, such as Ga_{Zn}–O_i and Ga_{Zn}–V_{Zn} or the formation of Ga related oxide phases, such as Ga_2O_3, resulting in intense nonradiative recombination.[20, 21] In impurity-doped semiconductors, excess doping deteriorates effects of deep level emission. Figure 4(d) shows the change in the centered position of deep level emission in GZO nanorods. The GZO nanorods synthesized at low temperatures show deep level emission centered at ~2.5 eV. With increasing growth temperature, the position of the deep level emission exhibited a continuous shift toward a low energy level (2.2 eV at 900 °C). In a previous study,[22] the deep level emission at ~2.5 eV was attributed to oxygen vacancies, which is the normal emission peak in nanorods fabricated using vapor-transfer methods. It was suggested that the peaks at ~2.3 eV correspond to Ga impurity in heavily Ga-doped ZnO layers. This indicates that the deep-level emission observed in the GZO nanorods synthesized at high temperatures may due to the excess incorporation of Ga atoms.[11] In contrast, the medium temperature of 700~800 °C induced lower deep-emission intensity relative to NBE, which means that the ZnO nanorods were successfully doped with Ga atoms.

In order to examine the effect of different synthesis temperatures on the electrical characteristics of GZO nanorods, the *I*–*V* curves of the *n*-type GZO nanorods were obtained after forming a metal contact on the top region of the GZO nanorods. Figure 5(a) presents a schematic diagram of the structure used for the electrical measurements. Although this method does not show the characteristics of the nanorods directly, comparative analysis of the electrical conductivity of the GZO nanorods can be performed from the gradient of the *I*–*V* curve on *n*-type conducting GZO nanorods/*n*-type semiconducting ZnO films, as described elsewhere.[13] All *I*–*V* curves showed Ohmic-like linear behavior between the two Au/Ti metal electrodes on the GZO nanorods because the device structure consisted of only *n*-type semiconducting films, and there is no energy barrier between the GZO nanorods and ZnO template. The electrical resistance of the nanorods in the GZO nanorods/ZnO film structures can be indirectly compared, since we used the same ZnO films, where the GZO nanorods/ZnO films synthesized at 600, 700, 800, and 900 °C showed 2.5×10^4, 1.6×10^4, 1.2×10^3, and 4.8×10^3 Ω, respectively, with from *I*–*V* curves. With increasing synthesis temperature, the GZO nanorods became more conducting up to 800 °C but their electrical conductivity decreased significantly with further increases in temperature. Some groups reported the enhancement in electrical conductivity of Ga-doped ZnO nanorods compared to undoped ZnO nanorods.[10, 13] Therefore, it is expected that the highly conducting GZO nanorods were synthesized at 800 °C. However, higher synthesis temperature shows less conductive nanorods, implying the increase of the electrically inactive dopants. This behavior showed similar trends to the PL results.

Delivered by Ingenta to: Sung Kyun Kwan University IP: 115.145.205.35 Mon, 10 Jan 2011 09:24:17

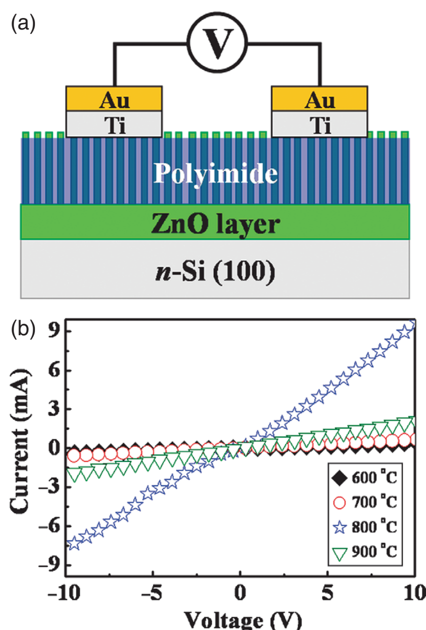

Fig. 5. (a) Schematic diagram of the GZO nanorods/template/*n*-Si structure for the electrical measurements. (b) The *I*–*V* curves of these structures as function of the growth temperature.

4. SUMMARY

Vertically aligned GZO nanorods were produced on a ZnO template using simple thermal evaporation at various temperatures. The effect of the synthesis temperature on the chemical, electrical, and structural properties in the GZO nanorods were examined. With increasing synthesis temperature up to 800 °C, the growth rate was quite rapid, the intensity of NBE emission became stronger, and the electrical properties became more conducting. At the lower temperature regions, the GZO nanorods showed less compressive strain, due to the elimination of defects enhancing stress. This means that stress makes a more dominant contribution than the doping effect. On the other hand, synthesis at 900 °C induced the formation of shorter and less conducting nanorods, together along weak NBE emission.

Acknowledgments: This work was supported by the National Research Foundation of Korea(NRF) grant funded by the Korea government (MEST) (2009-0078876).

RESEARCH ARTICLE

The National Research Foundation of Korea (NRF) funded by the Ministry of Education, Science and Technology (2009-0083009).

References and Notes

1. M. H. Huang, S. Mao, H. Feick, H. Q. Yan, Y. Y. Qu, H. Kind, E. Weber, R. Russo, and P. D. Yang, *Science* 292, 1897 **(2001)**.
2. J. G. Lu, Z. Z. Ye, G. D. Yuan, Y. J. Zeng, F. Zhuge, L. P. Zhu, B. H. Zhao, and S. B. Zhang, *Appl. Phys. Lett.* 89, 053501 **(2006)**.
3. E. M. C. Fortunato, P. M. C. Barquinha, A. C. M. B. G. Pimentel, A. M. F. Goncalves, A. J. S. Marqures, R. F. P. Martins, and L. M. N. Pereira, *Appl. Phys. Lett.* 85, 2541 **(2004)**.
4. R. Ramanoorthy, P. K. Dutta, and S. A. Akbar, *J. Mater. Sci.* 38, 4271 **(2003)**.
5. J. Zhou, Y. Gu, P. Fei, W. Mai, Y. Gao, R. Yang, G. Bao, and Z. L. Wang, *Nano Lett.* 8, 3035 **(2008)**.
6. G. C. Yi, C. Wang, and W. II Park, *Semicond. Sci. Technol.* 20, S22 **(2005)**.
7. X. Y. Xue, L. M. Li, H. C. Yu, Y. J. Chen, Y. G. Wang, and T. H. Wang, *Appl. Phys. Lett.* 89, 043118 **(2006)**.
8. C. L. Hsin, J. H. He, and L. J. Chen, *Appl. Phys. Lett.* 88, 063111 **(2006)**.
9. J. Zhong, S. Muthukumar, Y. Chen, Y. Lu, H. M. Ng, W. Jiang, and E. L. Garfunkel, *Appl. Phys. Lett.* 83, 3401 **(2003)**.
10. C. Xu, M. Kim, J. Chun, and D. Kim, *Appl. Phys. Lett.* 86, 133107 **(2005)**.
11. H. J. Ko, Y. F. Chen, S. K. Hong, H. Wenisch, T. Yao, and D. C. Look, *Appl. Phys. Lett.* 77, 3761 **(2000)**.
12. T. Yamada, A. Miyake, S. Kishimoto, H. Makino, N. Yamamoto, and T. Yamamoto, *Appl. Phys. Lett.* 91, 051915 **(2007)**.
13. C. H. Ahn, W. S. Han, B. H. Kong, and H. K. Cho, *Nanotechnology* 20, 015601 **(2009)**.
14. R. C. Wang, C. P. Liu, J. L. Huang, and S. J. Chen, *Appl. Phys. Lett.* 88, 023111 **(2006)**.
15. C. X. Xu, X. W. Sun, and B. J. Chen, *Appl. Phys. Lett.* 84, 1540 **(2004)**.
16. X. H. Wang, X. W. Fan, C. X. Shan, Z. Z. Zhang, J. Y. Zhang, Y. M. Lu, Y. C. Liu, D. Z. Shen, Y. K. Su, and S. Chang, *J. Mater. Chem. Phys.* 88, 102 **(2004)**.
17. J. W. Shin, J. Y. Lee, T. W. Kim, Y. S. No, W. J. Cho, and W. K. Choi, *Appl. Phys. Lett.* 88, 091911 **(2006)**.
18. S. M. Park, T. Ikegami, and K. Ebihara, *Thin Solid Films* 513, 90 **(2006)**.
19. H. C. Park, D. Byun, B. Angadi, D. H. Park, W. K. Choi, and J. W. Choi, *J. Appl. Phys.* 102, 073114 **(2007)**.
20. H. Matsui, H. Saeki, H. Tabata, and T. Kawai, *J. Electrochem. Soc.* 150, G508 **(2003)**.
21. N. Roberts, R. P. Wang, A. W. Sleight, and W. W. Warren, *Phys. Rev. B* 57, 5734 **(1998)**.
22. C. H. Ahn, Y. Y. Kim, D. C. Kim, S. K. Mohanta, and H. K. Cho, *J. Appl. Phys.* 105, 013502 **(2009)**.

Received: 20 July 2009. Accepted: 28 December 2009.

Delivered by Ingenta to:
Sung Kyun Kwan University
IP : 115.145.205.35
Mon, 10 Jan 2011 00:24:17